bioRxiv preprint doi: https://doi.org/10.1101/2020.11.13.381434; this version posted March 3, 2021. The copyright holder for this preprint (which was not certified by peer review) is the author/funder. All rights reserved. No reuse allowed without permission.

RNA polymerase backtracking results in the accumulation of fission yeast condensin at active genes.

Julieta Rivosecchi[1,2,†], Daniel Jost[1,†], Laetitia Vachez[1], François Gautier[1], Pascal Bernard[1] and Vincent Vanoosthuyse[1,*]

1. Univ Lyon, École Normale Supérieure de Lyon, CNRS, UMR 5239, Laboratoire de Biologie et Modélisation de la Cellule, 46 allée d'Italie F-69364 LYON, France.
2. *Present address* : Department of Cellular, Computational and Integrative Biology – CIBIO. University of Trento. Via Sommarive, 9. 38123 - Trento, Italy

† Equal contribution

* For correspondence : vincent.vanoosthuyse@ens-lyon.fr

Running title: RNAP backtracking and condensin buildup.

Keywords: chromosomes, condensin, RNAP backtracking, Sen1, SMC, transcription

bioRxiv preprint doi: https://doi.org/10.1101/2020.11.13.381434; this version posted March 3, 2021. The copyright holder for this preprint (which was not certified by peer review) is the author/funder. All rights reserved. No reuse allowed without permission.

Summary blurb (<200 characters; 185):

Using both experiments and mathematical modelling, the authors show that RNA Polymerase backtracking contributes to the accumulation of condensin in the termination zone of active genes.

Abstract (175 words max; 170)

The mechanisms leading to the accumulation of the SMC complexes condensins around specific transcription units remain unclear. Observations made in bacteria suggested that RNA polymerases (RNAP) constitute an obstacle to SMC translocation, particularly when RNAP and SMC travel in opposite directions. Here we show in fission yeast that gene termini harbour intrinsic condensin-accumulating features whatever the orientation of transcription, which we attribute to the frequent backtracking of RNAP at gene ends. Consistent with this, to relocate backtracked RNAP2 from gene termini to gene bodies was sufficient to cancel the accumulation of condensin at gene ends and to redistribute it evenly within transcription units, indicating that RNAP backtracking may play a key role in positioning condensin. Formalization of this hypothesis in a mathematical model suggests that the inclusion of a sub-population of RNAP with longer dwell-times is essential to fully recapitulate the distribution profiles of condensin around active genes. Taken together, our data strengthen the idea that dense arrays of proteins tightly-bound to DNA alter the distribution of condensin on chromosomes.

bioRxiv preprint doi: https://doi.org/10.1101/2020.11.13.381434; this version posted March 3, 2021. The copyright holder for this preprint (which was not certified by peer review) is the author/funder. All rights reserved. No reuse allowed without permission.

INTRODUCTION

Structural Maintenance of Chromosomes (SMC) complexes are essential for the organization and stability of chromosomes from bacteria to humans (Hassler *et al*, 2018; van Ruiten & Rowland, 2018; Uhlmann, 2016). The SMC complex condensin is particularly important for the compaction and the structuration of chromosomes throughout mitosis and for their faithful segregation to daughter cells (Hirano, 2016). Condensin is a ring-shaped DNA translocase that uses the energy of ATP-hydrolysis to organize mitotic chromosomes into large consecutive loops of chromatin (Naumova *et al*, 2013; Gibcus *et al*, 2018). It has been shown *in vitro* that purified condensin hydrolyses ATP to extrude loops of naked DNA (Kong *et al*, 2020; Ganji *et al*, 2018), but the structural details of the formation and enlargement of such loops remain poorly understood (Cutts & Vannini, 2020). Furthermore, whether such loop extrusion activity is the only way that condensin complexes organize mitotic chromosomes is still under debate as condensins and other architectural proteins may also participate in the organization of chromosomes by bridging-induced phase separation (Cheng *et al*, 2015; Sakai *et al*, 2018; Ryu *et al*, 2021)).

Another fundamental question is to understand how chromatin and large DNA-bound protein assemblies impact the loop extrusion activity of condensin *in vivo*. Loop extrusion on chromatin *in vivo* is predicted to be roughly 10 times slower than on naked DNA *in vitro* (Banigan & Mirny, 2020) and it was recently suggested that arrays of proteins tightly bound to DNA could hinder the loop extrusion activity of condensin, possibly by constituting a steric obstacle to the reeling of chromatin (Guérin *et al*, 2019). An inability to bypass obstacles might result in the formation of unlooped chromatin gaps within mitotic chromosomes (Banigan *et al*, 2020). Whether and how condensin bypasses chromatin-associated obstacles is currently unclear.

Gene transcription has been shown to influence the distribution of SMC complexes in several organisms. In *Bacillus subtilis* and *Caulobacter crescentus*, a single SMC complex juxtaposes the arms of a circular chromosome by translocating in a unidirectional fashion from a single loading site (Tran *et al*, 2017; Wang *et al*, 2015; Le *et al*, 2013; Sullivan *et al*, 2009; Gruber & Errington, 2009). A highly active transcription unit in the opposite direction (head-on orientation) was shown to slow down the translocation of SMC, which transiently accumulates towards the 3' of the unit in a transcription-dependent manner (Brandão *et al*, 2019; Tran *et al*, 2017; Wang *et al*, 2017). It has been proposed that RNA polymerase (RNAP) molecules themselves constitute a directional albeit permeable barrier that impedes the translocation of SMC and each encounter with a RNAP molecule would force SMC to stall for a few seconds (Brandão *et al*, 2019). Great densities of RNAP (or other DNA-bound proteins) are therefore expected to impact the distribution of SMC along chromosome arms. Interestingly, specific mutations in *B. subtilis* SMC were shown to interfere with its ability to overcome transcription-dependent obstacles, suggesting that their bypass is an active process (Vazquez Nunez *et al*, 2019). Consistent with this, it was postulated that the bypass rate of different SMC complexes is a function of their intrinsic ATP hydrolysis rates (Brandão *et al*, 2019). In eukaryotes, transcription is also a positioning device for the SMC complex cohesin in interphase (Heinz *et al*, 2018; Busslinger *et al*, 2017; Bausch *et al*, 2007; Lengronne *et al*, 2004), suggesting that transcription is a conserved regulator of SMC occupancy.

Transcription also impinges on the distribution of condensin complexes in eukaryotes, even in organisms where active transcription is strongly reduced in mitosis when the association of condensin with chromosomes is the strongest (Bernard & Vanoosthuyse, 2015). In both chicken and human cells, condensin I, which only associates with predominantly transcriptionally-silent chromatin after nuclear envelope breakdown in mitosis, accumulates towards the 5' of RNAP2-transcribed genes that were highly transcribed in the previous G2 phase (Kim *et al*, 2013; Sutani *et al*, 2015). Similarly, in mouse ES cells and human cells, the localisation of condensin II, which is nuclear throughout the cell cycle, correlates with RNAP2 occupancy, and human condensin II accumulates at the 3' end of highly transcribed genes in interphase cells (Dowen *et al*, 2013; Iwasaki *et al*, 2019). By contrast, RNAP1 transcription

bioRxiv preprint doi: https://doi.org/10.1101/2020.11.13.381434; this version posted March 3, 2021. The copyright holder for this preprint (which was not certified by peer review) is the author/funder. All rights reserved. No reuse allowed without permission.

was proposed to antagonize the accumulation of condensin within the 35S transcription unit in budding yeast (Clemente-Blanco *et al*, 2009; Johzuka & Horiuchi, 2007). The role of transcription in establishing condensin-accumulating regions is therefore unclear. Fission yeast is a very good model to understand how transcription affects condensin because transcription remains active during mitosis, when the activity of condensin is maximal. A number of studies have established that fission yeast condensin accumulates in a transcription-dependent manner in the vicinity of genes that are highly expressed in mitosis, whatever the RNA polymerase involved (RNAP1, RNAP2 or RNAP3) (Kim *et al*, 2016; Sutani *et al*, 2015; Nakazawa *et al*, 2015; Kim *et al*, 2014; Nakazawa *et al*, 2008). Moreover, the drug-induced inhibition of transcription partially rescued the loss of viability of condensin-defective mutants (Sutani *et al*, 2015) and it was recently proposed that active transcription interferes locally with the condensin-dependent resolution of sister chromatids (Nakazawa *et al*, 2019b). Taken together, these observations suggest that transcriptionally active RNA polymerases, and/or features associated with ongoing transcription, might challenge condensin function and the assembly of mitotic chromosomes in fission yeast.

We have previously proposed that fission yeast condensin might load onto DNA at nucleosome-depleted promoters of active genes (Toselli-Mollereau *et al*, 2016) and would subsequently accumulate particularly towards the 3' of genes actively transcribed by RNAP2 (Toselli-Mollereau *et al*, 2016; Sutani *et al*, 2015). Considering the relatively small size of transcription units in fission yeast (~2 kb for protein-coding genes), a condensin complex loaded at the promoter might be more likely to reach the 3' of genes in a head-to-tail than in a head-to-head orientation. It is therefore unclear whether the accumulation of condensin in the 3' of genes is due to a head-on conflict between transcription and translocating condensin, like in bacteria (see above). On the other hand, there is evidence that the positioning of fission yeast condensin at the 3' of RNAP2-transcribed genes could be functionally linked to the process of transcription termination. First, a number of positive and negative genetic interactions have been reported between mutants of the transcription termination machinery and mutants of condensin (Nakazawa *et al*, 2019a; Vanoosthuyse *et al*, 2014). As lack of condensin does not directly impact transcription termination in fission yeast (Nakazawa *et al*, 2019a; Hocquet *et al*, 2018), these genetic interactions suggest that RNAP2 transcription termination mechanisms might impinge on the function of condensin. Consistent with this interpretation, it was shown recently that to inactivate $Xrn2^{Dhp1}$, an enzyme that is key for RNAP2 transcription termination, was sufficient to displace condensin further downstream of active transcription units (Nakazawa *et al*, 2019a), strengthening the possibility of interplay between transcription termination mechanisms, the 3' edge of the RNAP2 domain and the positioning of condensin. To explain these observations, it was proposed that condensin is actively recruited at transcription termination regions because they accumulate single-stranded DNA (ssDNA) and/or chromatin-associated RNA molecules that interfere with the organization of mitotic chromosomes (Nakazawa *et al*, 2019a; Sutani *et al*, 2015). Condensin, thanks to its ability to re-anneal melted dsDNA molecules *in vitro* (Sutani *et al*, 2015; Akai *et al*, 2011; Sakai *et al*, 2003; Sutani & Yanagida, 1997), would suppress these structures, thereby allowing the formation of fully functional mitotic chromosomes. This hypothesis therefore posits that condensin plays a "clearing" role in the assembly of mitotic chromosomes (Yanagida, 2009) besides its role in the extrusion of chromatin loops. It remains unclear however how short chromosome regions that are rich in single-stranded DNA (ssDNA) and/or chromatin-associated RNA could interfere with the formation of segregation-competent mitotic chromosomes. Importantly, other models could also account for these observations: (i) a permeable moving barrier model as described in bacteria (Brandão *et al*, 2019) could explain the accumulation of translocating condensin at the 3' border of the RNAP2 domain or (ii) the transcription termination machinery could play a more direct role in the positioning of moving condensin. These models haven't yet been tested experimentally.

Here we sought to better understand what features of transcription might influence the distribution of condensin in fission yeast mitosis. By switching the orientation of an RNAP2-

bioRxiv preprint doi: https://doi.org/10.1101/2020.11.13.381434; this version posted March 3, 2021. The copyright holder for this preprint (which was not certified by peer review) is the author/funder. All rights reserved. No reuse allowed without permission.

transcribed gene expressed in mitosis, we tested whether or not gene transcription could be a directional barrier for condensin. Although these experiments neither confirmed nor infirmed that transcription might be a directional barrier in fission yeast, they strongly reinforced the idea that the 3' end of genes contain intrinsic condensin-positioning features. We then showed that to interfere with RNAP3 transcription termination also alters the distribution of condensin, suggesting that transcription termination defects impact the accumulation of condensin, whatever the RNA polymerase involved. This strengthened the idea that RNAP molecules rather than a specific transcription termination machinery could influence the positioning of condensin. Consistent with this, we provide evidence that to increase the stability of backtracked RNAP2 polymerases throughout the gene body was sufficient to shift condensin occupancy towards the 5' end of transcribed genes. This strongly suggests that backtracked RNA polymerase molecules are themselves positioning devices for condensin. We used mathematical modelling to formalize this hypothesis and determined that simulations that take into account the presence of two distinct RNAP populations, one mobile and one backtracked, more closely predict the distribution pattern of condensin around active genes in fission yeast than those that only consider the mobile population of RNAP, as previously described (Brandão *et al*, 2019). Taken together, our data clarify the role of transcription in the accumulation of condensin and are consistent with the idea that proteins that are tightly-bound to DNA impact the distribution of condensin along mitotic chromosomes.

RESULTS

One prediction of the permeable moving barrier model is that the orientation of transcription impacts the distribution pattern of condensin (Brandão *et al*, 2019). To test this prediction in fission yeast, we changed the orientation of *exg1*, a gene that is transcribed by RNAP2 in mitosis and where condensin was shown previously to accumulate strongly towards the termination zone (Kakui *et al*, 2017) (Fig 1A). Interestingly, it was shown that RNAP2 levels remain relatively constant throughout the gene (Sutani *et al*, 2015) (Fig 1A), arguing that the density of RNAP2 *per se* is unlikely to account for the position of condensin at the 3' end of this gene. Importantly, the reversal of orientation did not affect RNAP2 levels around *exg1* in mitotic cells (Fig 1BC). Strikingly, the peak of condensin accumulation was moved symmetrically with the flipping of *exg1* and coincided with the new genomic position of the 3' end of the gene (Fig 1BC). These observations could be interpreted in several ways: either (i) transcription is not a directional barrier for condensin in fission yeast, or (ii) transcription is a directional barrier for condensin but the chromatin around *exg1* can be reeled by condensin from both directions with equal probability; alternatively, (iii) the transcription termination process itself or its machinery forces the accumulation of condensin in the 3' end of transcribed genes.

To test the latter hypothesis, we assessed whether transcription termination at another class of genes also modulates the distribution of condensin. Several ChIP-seq studies reported that fission yeast condensin accumulates at RNAP3-transcribed genes (Kakui *et al*, 2017; Kim *et al*, 2016; Sutani *et al*, 2015; Kim *et al*, 2014) and it was proposed that the B-box binding transcription factor TFIIIC and the TATA-binding protein Tbp1 were required for this accumulation by interacting directly with condensin (Iwasaki *et al*, 2015, 2010). Whether or not transcription termination at RNAP3-transcribed genes could impact the distribution of condensin was not investigated. We recently demonstrated that the conserved DNA&RNA helicase Sen1 is required for efficient transcription termination at RNAP3-transcribed genes in -*cis* (Rivosecchi *et al*, 2019). In the absence of Sen1, RNAP3 strongly accumulates downstream of most of its target genes and we showed that this accumulation of read-through RNAP3 molecules downstream of gene ends could be suppressed by strengthening the endogenous terminators by the use of long polyT sequences (Rivosecchi *et al*, 2019). We tested whether the RNAP3 termination defects associated with lack of Sen1 could impact the distribution of condensin around RNAP3-transcribed genes. Strikingly, condensin levels increased significantly at a subset of RNAP3-transcribed genes in synchronized mitotic cells lacking Sen1 (Fig 2A). This accumulation was specific because lack of Sen1 had no impact on

bioRxiv preprint doi: https://doi.org/10.1101/2020.11.13.381434; this version posted March 3, 2021. The copyright holder for this preprint (which was not certified by peer review) is the author/funder. All rights reserved. No reuse allowed without permission.

the association of the heterologous *E. coli* protein LacI expressed in fission yeast cells (Fig 2A). Importantly, the accumulation of condensin in *sen1*Δ cells could not be caused by an accumulation of either TFIIIC or Tbp1, because their levels on chromatin remained largely unaffected in the absence of Sen1, as shown by ChIP with a GFP-tagged version of Tbp1 and a myc-tagged version of the TFIIIC component Sfc6 (Fig 2B and Supplementary Fig S1). In the absence of Sen1, condensin did not accumulate either at COC sites (Fig 2A), which recruit TFIIIC but not RNAP3 (Noma *et al*, 2006), consistent with a transcription-mediated effect. To further determine whether the accumulation of condensin was mechanistically linked to the transcription termination defects observed in the absence of Sen1, we corrected those defects by strengthening the terminator sequences at two tRNA genes by inserting long polyT sequences, as described previously (Rivosecchi *et al*, 2019). As expected, this strategy was sufficient to correct the accumulation of RNAP3 downstream of the terminator sequences in mitotic cells lacking Sen1 (Fig 2CD, lower panels). Strikingly, this was also sufficient to prevent the accumulation of condensin (Fig 2CD, top panels). These observations show that the increased accumulation of condensin at class III genes in the absence of Sen1 is a direct consequence of RNAP3 transcription termination defects. This is reminiscent of the data showing that to interfere with RNAP2 transcription termination mechanisms also altered the distribution of condensin (Nakazawa *et al*, 2019a) or cohesin (Heinz *et al*, 2018) in *-cis*. As the transcription termination machineries differ for RNAP2 and RNAP3, it seems unlikely that a component of the transcription termination machinery itself is involved in the positioning of condensin in the 3' of genes. Our data suggest instead that intrinsic properties of RNA polymerase molecules undergoing a termination process might explain their impact on the distribution of condensin.

What could be the intrinsic properties of RNAP molecules in the 3' end of genes that impact the position of condensin? We hypothesized that RNAP backtracking could be a contributing factor for two reasons: (i) RNAP molecules are often backtracked around termination sites (Sheridan *et al*, 2019; Lemay *et al*, 2014) and (ii) backtracking would conceivably strengthen the interaction of RNAP molecules with chromatin, making them less dynamic and possibly a harder obstacle to bypass by translocating condensin molecules (Guérin *et al*, 2019; Brandão *et al*, 2019). To test this hypothesis, we sought to prolong RNAP2 backtracking events by over-expressing a dominant-negative mutant of TFIIS (*tfs1D274AE275A* in fission yeast (Lemay *et al*, 2014), thereafter referred to as *tfs1DN*). This strategy was shown to interfere with transcription elongation throughout the gene in different organisms and to alter the distribution of RNAP2 (Zatreanu *et al*, 2019; Sheridan *et al*, 2019; Sigurdsson *et al*, 2010). Upon *tfs1DN* expression in mitotic fission yeast cells, the distribution of RNAP2 was reduced in the 3' and shifted towards the 5' of genes (Fig 3). Remarkably, the over-expression of *tfs1DN* had a similar impact on the distribution of condensin around RNAP2-transcribed genes in mitosis (Fig 3): the accumulation of condensin at the 3' of genes was significantly reduced but its accumulation towards the 5' increased significantly. Overall, condensin became evenly distributed throughout the gene body upon *tfs1DN* over-expression instead of being enriched at the transcription termination site. On the contrary, over-expression of *tfs1DN* had no impact on the association of condensin with the RNAP1-transcribed 18S (Supplementary Fig S2). Taken together, these observations are consistent with the idea that RNAP backtracking impacts the distribution of condensin within transcribed genes. Because backtracking is a prominent feature in the 3' end of genes (Sheridan *et al*, 2019; Lemay *et al*, 2014), this might explain why condensin accumulates particularly over the 3' of transcriptionally active genes in fission yeast (Toselli-Mollereau *et al*, 2016; Sutani *et al*, 2015).

To challenge this hypothesis, we used mathematical modelling of the interplay between condensin and RNAP (Fig 4, Supplementary Fig S3, Supplementary Fig S4 and Supplementary Text). Previous models assumed that RNAP could push condensin towards the 3' of the gene and that condensin could bypass RNAP after a small delay (Brandão *et al*, 2019). We first implemented this model (Fig 4A) and confirmed that it predicts an accumulation of condensin in the 3' of genes if RNAP and condensin travel in opposite directions (Fig 4BC),

bioRxiv preprint doi: https://doi.org/10.1101/2020.11.13.381434; this version posted March 3, 2021. The copyright holder for this preprint (which was not certified by peer review) is the author/funder. All rights reserved. No reuse allowed without permission.

as reported previously (Brandão *et al*, 2019). Importantly, this predicted accumulation followed an almost exponential profile through the gene (Fig 4C and (Brandão *et al*, 2019)), which does not correspond to what is observed *in vivo* for fission yeast condensin or for human condensin II, where the accumulation of condensin increases gradually and slowly in the gene body with an additional strong peak around the termination zone (Fig 1&3 and (Sutani *et al*, 2015; Iwasaki *et al*, 2019)). We conclude that this first model cannot fully recapitulate observations made *in vivo*.

Importantly, this first model considered that all RNAP molecules have the same properties and the same dynamics throughout the transcription unit. This however does not correspond to the reality of the transcription cycle, where RNAP frequently pauses and backtracks, notably in the termination zone (reviewed in (Noe Gonzalez *et al*, 2021). We therefore built a second model (Fig 4D), where RNAP may dynamically switch between an elongating, mobile form (in orange on Fig 4D) and a backtracked, immobile state (in red on Fig 4D). As in the previous model (Brandão *et al*, 2019), we considered that mobile RNAP molecules can push condensin towards the 3' of the gene. In addition, we postulated that bypassing backtracked RNAPs is less efficient (Fig 4D). In normal conditions, the major site of RNAP backtracking would be the termination zone (Fig 4EF). Importantly, as is observed *in vivo,* this second model predicted a gradual accumulation of condensin in the body of genes and a more pronounced accumulation in the termination zone (Fig 4G). Strikingly, the model made those predictions whatever the direction of travel of condensin (co-directional, full black line, or head-on, dotted black line, Fig 4G). This is reminiscent of our observations that flipping *exg1* did not fundamentally change the distribution pattern of condensin (Fig 1).

We tested our model to see whether it could predict the changes to the distribution of condensin triggered by the over-expression of *tfs1DN* (Fig 3). In this situation, we assumed that the dwell-time of the backtracked state is strongly increased. As a result, the proportion of backtracked RNAP significantly increases inside the gene body and the global RNAP occupancy is shifted towards the 5' of the gene (Fig 4H). Strikingly, our new model predicted that condensin would accumulate more evenly throughout the gene body in those conditions and lose its specific accumulation in the termination zone (Fig 4I). This is in perfect agreement with our observations *in vivo* (Fig 3). We conclude that accounting for the presence of backtracked RNAP along the gene is a key ingredient to describe the pattern of condensin around active genes.

DISCUSSION

Taken together, our results strongly suggest that RNAP backtracking results in the accumulation of condensin in -*cis*. This could explain why both yeast condensin (this study and (D'Ambrosio *et al*, 2008; Sutani *et al*, 2015)) and human condensin II (Iwasaki *et al*, 2019) tend to accumulate in the 3' of active genes. Our data also confirm that to interfere with transcription elongation affects the distribution of condensin within genes (Fig 3), as predicted previously (Brandão *et al*, 2019). In the future, single molecule approaches could be used to determine experimentally whether condensin pauses for longer when facing backtracked RNAP molecules than when facing elongating, dynamic RNAP.

In the absence of Sen1, RNAP3 accumulates strongly over and downstream of class III genes but this accumulation is associated with reduced rates of transcription (Rivosecchi *et al*, 2019). We therefore speculate that those accumulated RNAP3 molecules are often backtracked and that the increased levels of condensin downstream of class III genes in the absence of Sen1 depend on the size and the density of the domain occupied by these read-through, backtracked polymerases. By introducing super-terminator sequences (Fig 2), we reduced the size of this domain and prevented the accumulation of condensin. Both the size and the density of this RNAP3-rich read-through domain would depend on the chromatin context and the transcription rate. This might explain why condensin did not accumulate at all RNAP3-transcribed genes in the absence of Sen1 (Fig 2). Note also that in our hands, RNAP3-transcribed genes are not strong condensin-accumulation sites when Sen1 is present (Fig 2) and we predict that this is because the size of the domain occupied by RNAP3 and TFIIIC is not large enough to constitute a significant obstacle (~100 bp).

bioRxiv preprint doi: https://doi.org/10.1101/2020.11.13.381434; this version posted March 3, 2021. The copyright holder for this preprint (which was not certified by peer review) is the author/funder. All rights reserved. No reuse allowed without permission.

Our data are also consistent with the observation that the number and density of DNA-bound Rap1 proteins influence condensin function in budding yeast (Guérin *et al*, 2019) and strengthen the idea that arrays of proteins that are tightly-bound to DNA could trigger the accumulation of condensin. Similarly, it is conceivable that a number of tightly-bound proteins (for example transcription factors or paused RNAP2 molecules) contribute to position condensin I in the 5' of genes in mitosis in vertebrates (Sutani *et al*, 2015; Kim *et al*, 2013), even in the absence of significant transcriptional activity. We predict that the same rules are likely to apply to other SMC complexes.

It remains to be determined why tightly-bound proteins lead to the accumulation of condensin. They might represent regions where condensin is preferentially loaded but we favor the idea that they might oppose steric hindrance to the translocation of condensin, as argued previously (Guérin *et al*, 2019). Alternatively, they might modify the local physical properties of the chromatin fibre or some properties of condensin itself in a way that would eventually challenge its translocation. Future work is needed to answer these important questions and to understand better how condensin and other SMC complexes work in the context of chromatin.

MATERIAL AND METHODS

Yeast strains. The strains used in this study are listed on Supplementary Table S1.

Cell synchronization. Two different methods were used to synchronize fission yeast cells in metaphase. The first method (Fig 1BC and Fig 2CD) used an analogue-sensitive version of the Cyclin-DK Cdc2 (*cdc2-asM17*, (Aoi *et al*, 2014)) which can be inhibited by 2 µM of 3-Br-PP1 (A602985, Toronto Research Chemicals). After 3 hours in the presence of the drug at 28°C in rich medium, 5.10^8 cells were filtered, washed 3 times with warm medium and released in fresh medium without BrPP1. After 10 minutes, ~80% of cells were in mitosis, as judged by the localization of GFP-tagged condensin (Cnd2) in the nucleus. The second synchronization method (Fig 2AB and Fig 3) relies on the inhibition of the expression of Slp1 (Petrova *et al*, 2013), a protein that is key to the metaphase to anaphase transition (Matsumoto, 1997). Cells expressing Slp1 under the control of the thiamine-repressible *nmt41* promoter were grown in minimal medium at 32°C until mid-log phase, when 60 µM of thiamine was added to the culture for 3 hours. Cell synchrony in mitosis was checked as above by the presence of GFP-tagged condensin (Cnd2) in the nucleus.

***Exg1* inversion.** *ura4* was first integrated at the *exg1* locus to generate the *exg1*Δ::ura4+ strain. PCR was then used to fuse the 3' of *exg1* to its 5' domain and its 5' to its 3' domain using the primers exg1 qL2/exg1 RV3 and exg1 qR2/exg1 FW3 (see Supplementary Table S2 for a list of the primers used in this study). An overlapping PCR was then used to amplify the whole inverted locus. The resulting 2.8 kb PCR product was then transformed into the *exg1*Δ*::ura4*+ strain and stable integrants were selected by several rounds of FOA selection. The correct integration of the *exg1* gene in the reverse orientation was confirmed by PCR and sequencing.

***tfs1DN* over-expression.** The strains of interest were transformed with the pFB818 plasmid (a generous gift from François Bachand, University of Sherbrooke) that allows the inducible expression of *tfs1-DN* by addition of 7.5 µM of anhydrotetracycline hydrochloride (AhTET; Sigma-Aldrich, 94664), as described in (Lemay *et al*, 2014). AhTET was dissolved in DMSO. Cells were grown in PMG-Leu at 30°C until they reached a concentration of 5.10^6 cells/mL. AhTET or DMSO was added for 3 hours, at which point 60 µM of thiamine was added to repress the expression of Slp1 as above.

Chromatin Immunoprecipitation (ChIP). ChIP was carried out as described previously (Rivosecchi *et al*, 2019), using the primers listed in Supplementary Table S2. GFP-tagged

bioRxiv preprint doi: https://doi.org/10.1101/2020.11.13.381434; this version posted March 3, 2021. The copyright holder for this preprint (which was not certified by peer review) is the author/funder. All rights reserved. No reuse allowed without permission.

proteins were immuno-precipitated with the A11122 antibody (Thermo Fisher Scientific); Myc-tagged proteins were immuno-precipitated with the 9E10 antibody (Merck); Rpb1 was immunoprecipitated using the 8WG16 antibody (Merck).

Mathematical modelling and simulations (see also the Supplementary Text)

We considered a genomic locus of 10kbp that we modelled as a unidimensional array of *N=100* bins (1bin=100bp). This region contains a 2kbp-long gene between bin 1 and bin 20. We investigated the interplay between RNAP elongation and condensin translocation using two models.

The simple model (Fig 4A). This first model is similar to the one described in (Brandão *et al*, 2019). RNAP elongation is modelled as a totally asymmetric simple exclusion process (TASEP) (Derrida *et al*, 1992; Klumpp & Hwa, 2008; Dobrzynski & Bruggeman, 2009). After binding to the TSS (bin 1) at a rate γ_{init}, RNAP molecules elongate at a speed rate of v_{RNAP} along the gene from 5' to 3' and unbind at a rate γ_{term} when they reach the termination zone (bins≥20). Binding at TSS or translocation to the adjacent bin of one RNAP may occur only if the corresponding bin is not already occupied by another RNAP. Condensin translocation occurs either from 5' to 3' (bin 1 to 100, head-to-tail situation) or from 3' to 5' (bin 100 to 1, head-to-head situation). Condensin translocates at a speed rate v_c in the absence of adjacent RNAPs in the direction of movement. In the presence of an RNAP, the rate of translocation is reduced to v_{jump}. As in (Brandão *et al*, 2019), we posited that RNAP translocation is not affected by condensin but that condensin may be pushed towards the 3' by an adjacent translocating RNAP. For simplicity, we assumed that only one condensin is travelling at a time along the region.

The backtrack model (Fig.4D). This second model accounts for the backtracking of RNAP and its impact on condensin translocation. RNAP dynamics is modelled as a TASEP with pauses (Klumpp, 2011; Wang *et al*, 2014). RNAPs switch between two states: a mobile, elongating state (mRNAP) and a paused, backtracked state (bRNAP). Initiation, elongation and termination occur as in the simple model except that only mRNAPs can move and that only bRNAPs can unbind. Switching from mobile to paused states happen at rate $k_{back}(i)$ that may depend on the position *i*. bRNAPs become mobile at a homogeneous rate k_{on}. Condensin translocates as described in the simple model except that the bypassing rate now depends on the state of the adjacent RNAP (v_{jump}^{m} and v_{jump}^{b} for mRNAPs or bRNAPs, respectively).

Simulations. Both models were studied using the standard Gillespie algorithm (Gillespie, 1977) that simulates exact stochastic trajectories for systems of reaction rates. For a given model and parameter set, we simulated 10^5 different events for each type of condensin translocation (head-to-tail or head-to-head). One event was composed of two steps: (1) a first stage where only RNAP dynamics was simulated in order to reach a steady-state configuration for RNAPs. RNAP occupancy profiles shown in Fig 4B&F&H represent the steady-state probabilities to find a RNAP at a given position; (2) a second stage where one condensin is introduced at bin 1 for head-to-tail situations or at bin 100 for head-to-head ones and where the full system is simulated until the condensin reaches bin 100 or bin 1, respectively. During this second stage, we monitored the total time spent by condensin at each bin. Fig 4C&G&I gives the average of the residence time at a given position over the 10^5 different simulations.

Parameters. In the simple model (TASEP), we used $v_{RNAP} = 40$ bp/s (=0.4 bin/s), a typical speed rate for elongating RNAPs (Milo *et al*, 2010). $\gamma_{init} = 0.05$ RNAP/s and $\gamma_{term} = 0.4$ s^{-1} were chosen to obtain a WT-like dense and flat profile for RNAP occupancy. For condensin translocation, we chose $v_c = 1$ kbp/s, a typical loop extrusion rate observed *in vitro* (Banigan *et al*, 2020), and varied v_{jump} from 1 to 15 bp/s. In the backtrack model (TASEP with pauses), we used $v_{RNAP} = 40$ bp/s, $\gamma_{init} = 0.05$ RNAP/s, $\gamma_{term} = 0.2$ s^{-1}. $k_{back}(i)$ is given in Fig 4E, assuming a 200-fold stronger rate of backtracking in the termination zone. $k_{on} = 0.2$ s^{-1} to obtain a flat profile for RNAP occupancy in the WT case and $k_{on} = 0.02$ s^{-1} for a tilted profile in the *tfs1DN* case (Fig 4 H&I). Condensin-related parameters are given by $v_c = 1$ kbp/s, $v_{jump}^{m} = 15$ bp/s and a maximal impact of backtracked RNAPs with $v_{jump}^{b} = 0$. A more detailed description of the models can be found in the Supplementary Text.

bioRxiv preprint doi: https://doi.org/10.1101/2020.11.13.381434; this version posted March 3, 2021. The copyright holder for this preprint (which was not certified by peer review) is the author/funder. All rights reserved. No reuse allowed without permission.

DATA AVAILABILITY

The in-house Matlab script developed for simulating the mathematical models from this publication is available at https://github.com/physical-biology-of-chromatin/BackRNAP-Condensin.

ACKNOWLEDGMENTS.

We are very grateful to François Bachand (University of Sherbrooke) for sending the *tfs1-DN* over-expression plasmid. This work was supported by a "Chaire d'Excellence" (Project TRACC, CHX11) and by the PRCE project (19-CE12-0016-04) awarded to VV by the Agence Nationale pour la Recherche (ANR), and by the PRCE project (ANR-15-CE12-0002-01) and a "Projet Fondation ARC" (PJA 20191209370) awarded to PB by the Agence Nationale pour la Recherche (ANR) and the Fondation ARC pour la recherche sur le cancer, respectively. DJ acknowledges additional funding by the Agence Nationale pour la Recherche (ANR-18-CE12-0006-03, ANR-18-CE45-0022-01).

AUTHOR CONTRIBUTION

Conceptualization: VV; Formal analysis: JR, DJ and VV; Methodology: DJ; Funding acquisition: PB and VV; Investigation: JR, LV, FG and VV; Supervision: VV; Writing -original draft: VV; Writing -review&editing: JR, DJ, PB and VV.

CONFLICT OF INTEREST.

The authors declare that they have no conflict of interest

REFERENCES

Akai Y, Kurokawa Y, Nakazawa N, Tonami-Murakami Y, Suzuki Y, Yoshimura SH, Iwasaki H, Shiroiwa Y, Nakamura T, Shibata E, *et al* (2011) Opposing role of condensin hinge against replication protein A in mitosis and interphase through promoting DNA annealing. *Open Biol* 1: 110023

Aoi Y, Kawashima SA, Simanis V, Yamamoto M & Sato M (2014) Optimization of the analogue-sensitive Cdc2/Cdk1 mutant by in vivo selection eliminates physiological limitations to its use in cell cycle analysis. *Open Biol* 4: 140063

Banigan EJ, van den Berg AA, Brandão HB, Marko JF & Mirny LA (2020) Chromosome organization by one-sided and two-sided loop extrusion. *eLife* 9: e53558

Banigan EJ & Mirny LA (2020) Loop extrusion: theory meets single-molecule experiments. *Curr Opin Cell Biol* 64: 124–138

Bausch C, Noone S, Henry JM, Gaudenz K, Sanderson B, Seidel C & Gerton JL (2007) Transcription alters chromosomal locations of cohesin in Saccharomyces cerevisiae. *Mol Cell Biol* 27: 8522–8532

Bernard P & Vanoosthuyse V (2015) Does transcription play a role in creating a condensin binding site? *Transcription* 6: 12–16

bioRxiv preprint doi: https://doi.org/10.1101/2020.11.13.381434; this version posted March 3, 2021. The copyright holder for this preprint (which was not certified by peer review) is the author/funder. All rights reserved. No reuse allowed without permission.

Brandão HB, Paul P, van den Berg AA, Rudner DZ, Wang X & Mirny LA (2019) RNA polymerases as moving barriers to condensin loop extrusion. *Proc Natl Acad Sci U S A* 116: 20489–20499

Busslinger GA, Stocsits RR, van der Lelij P, Axelsson E, Tedeschi A, Galjart N & Peters J-M (2017) Cohesin is positioned in mammalian genomes by transcription, CTCF and Wapl. *Nature* 544: 503–507

Cheng TMK, Heeger S, Chaleil RAG, Matthews N, Stewart A, Wright J, Lim C, Bates PA & Uhlmann F (2015) A simple biophysical model emulates budding yeast chromosome condensation. *eLife* 4: e05565

Clemente-Blanco A, Mayán-Santos M, Schneider DA, Machín F, Jarmuz A, Tschochner H & Aragón L (2009) Cdc14 inhibits transcription by RNA polymerase I during anaphase. *Nature* 458: 219–222

Cutts EE & Vannini A (2020) Condensin complexes: understanding loop extrusion one conformational change at a time. *Biochem Soc Trans* 48: 2089–2100

D'Ambrosio C, Schmidt CK, Katou Y, Kelly G, Itoh T, Shirahige K & Uhlmann F (2008) Identification of cis-acting sites for condensin loading onto budding yeast chromosomes. *Genes Dev* 22: 2215–2227

Derrida B, Domany E & Mukamel D (1992) An exact solution of a one-dimensional asymmetric exclusion model with open boundaries. *J Stat Phys* 69: 667–687

Dobrzynski M & Bruggeman FJ (2009) Elongation dynamics shape bursty transcription and translation. *Proc Natl Acad Sci U S A* 106: 2583–2588

Dowen JM, Bilodeau S, Orlando DA, Hübner MR, Abraham BJ, Spector DL & Young RA (2013) Multiple structural maintenance of chromosome complexes at transcriptional regulatory elements. *Stem Cell Rep* 1: 371–378

Ganji M, Shaltiel IA, Bisht S, Kim E, Kalichava A, Haering CH & Dekker C (2018) Real-time imaging of DNA loop extrusion by condensin. *Science* 360: 102–105

Gibcus JH, Samejima K, Goloborodko A, Samejima I, Naumova N, Nuebler J, Kanemaki MT, Xie L, Paulson JR, Earnshaw WC, *et al* (2018) A pathway for mitotic chromosome formation. *Science* 359

Gillespie DT (1977) Exact stochastic simulation of coupled chemical reactions. *J Phys Chem* 81: 2340–2361

Gruber S & Errington J (2009) Recruitment of condensin to replication origin regions by ParB/SpoOJ promotes chromosome segregation in B. subtilis. *Cell* 137: 685–696

Guérin TM, Béneut C, Barinova N, López V, Lazar-Stefanita L, Deshayes A, Thierry A, Koszul R, Dubrana K & Marcand S (2019) Condensin-Mediated Chromosome Folding and Internal Telomeres Drive Dicentric Severing by Cytokinesis. *Mol Cell* 75: 131-144.e3

bioRxiv preprint doi: https://doi.org/10.1101/2020.11.13.381434; this version posted March 3, 2021. The copyright holder for this preprint (which was not certified by peer review) is the author/funder. All rights reserved. No reuse allowed without permission.

Hassler M, Shaltiel IA & Haering CH (2018) Towards a Unified Model of SMC Complex Function. *Curr Biol CB* 28: R1266–R1281

Heinz S, Texari L, Hayes MGB, Urbanowski M, Chang MW, Givarkes N, Rialdi A, White KM, Albrecht RA, Pache L, *et al* (2018) Transcription Elongation Can Affect Genome 3D Structure. *Cell* 174: 1522-1536.e22

Hirano T (2016) Condensin-Based Chromosome Organization from Bacteria to Vertebrates. *Cell* 164: 847–857

Hocquet C, Robellet X, Modolo L, Sun X-M, Burny C, Cuylen-Haering S, Toselli E, Clauder-Münster S, Steinmetz L, Haering CH, *et al* (2018) Condensin controls cellular RNA levels through the accurate segregation of chromosomes instead of directly regulating transcription. *eLife* 7: e38517

Iwasaki O, Tanaka A, Tanizawa H, Grewal SIS & Noma K-I (2010) Centromeric localization of dispersed Pol III genes in fission yeast. *Mol Biol Cell* 21: 254–265

Iwasaki O, Tanizawa H, Kim K-D, Kossenkov A, Nacarelli T, Tashiro S, Majumdar S, Showe LC, Zhang R & Noma K-I (2019) Involvement of condensin in cellular senescence through gene regulation and compartmental reorganization. *Nat Commun* 10: 5688

Iwasaki O, Tanizawa H, Kim K-D, Yokoyama Y, Corcoran CJ, Tanaka A, Skordalakes E, Showe LC & Noma K-I (2015) Interaction between TBP and Condensin Drives the Organization and Faithful Segregation of Mitotic Chromosomes. *Mol Cell* 59: 755–767

Johzuka K & Horiuchi T (2007) RNA polymerase I transcription obstructs condensin association with 35S rRNA coding regions and can cause contraction of long repeat in Saccharomyces cerevisiae. *Genes Cells Devoted Mol Cell Mech* 12: 759–771

Kakui Y, Rabinowitz A, Barry DJ & Uhlmann F (2017) Condensin-mediated remodeling of the mitotic chromatin landscape in fission yeast. *Nat Genet* 49: 1553–1557

Kim H-S, Mukhopadhyay R, Rothbart SB, Silva AC, Vanoosthuyse V, Radovani E, Kislinger T, Roguev A, Ryan CJ, Xu J, *et al* (2014) Identification of a BET family bromodomain/casein kinase II/TAF-containing complex as a regulator of mitotic condensin function. *Cell Rep* 6: 892–905

Kim JH, Zhang T, Wong NC, Davidson N, Maksimovic J, Oshlack A, Earnshaw WC, Kalitsis P & Hudson DF (2013) Condensin I associates with structural and gene regulatory regions in vertebrate chromosomes. *Nat Commun* 4: 2537

Kim K-D, Tanizawa H, Iwasaki O & Noma K-I (2016) Transcription factors mediate condensin recruitment and global chromosomal organization in fission yeast. *Nat Genet* 48: 1242–1252

Klumpp S (2011) Pausing and Backtracking in Transcription Under Dense Traffic Conditions. *J Stat Phys* 142: 1252–1267

bioRxiv preprint doi: https://doi.org/10.1101/2020.11.13.381434; this version posted March 3, 2021. The copyright holder for this preprint (which was not certified by peer review) is the author/funder. All rights reserved. No reuse allowed without permission.

Klumpp S & Hwa T (2008) Stochasticity and traffic jams in the transcription of ribosomal RNA: Intriguing role of termination and antitermination. *Proc Natl Acad Sci U S A* 105: 18159–18164

Kong M, Cutts EE, Pan D, Beuron F, Kaliyappan T, Xue C, Morris EP, Musacchio A, Vannini A & Greene EC (2020) Human Condensin I and II Drive Extensive ATP-Dependent Compaction of Nucleosome-Bound DNA. *Mol Cell* 79: 99-114.e9

Le TBK, Imakaev MV, Mirny LA & Laub MT (2013) High-resolution mapping of the spatial organization of a bacterial chromosome. *Science* 342: 731–734

Lemay J-F, Larochelle M, Marguerat S, Atkinson S, Bähler J & Bachand F (2014) The RNA exosome promotes transcription termination of backtracked RNA polymerase II. *Nat Struct Mol Biol* 21: 919–926

Lengronne A, Katou Y, Mori S, Yokobayashi S, Kelly GP, Itoh T, Watanabe Y, Shirahige K & Uhlmann F (2004) Cohesin relocation from sites of chromosomal loading to places of convergent transcription. *Nature* 430: 573–578

Matsumoto T (1997) A fission yeast homolog of CDC20/p55CDC/Fizzy is required for recovery from DNA damage and genetically interacts with p34cdc2. *Mol Cell Biol* 17: 742–750

Milo R, Jorgensen P, Moran U, Weber G & Springer M (2010) BioNumbers--the database of key numbers in molecular and cell biology. *Nucleic Acids Res* 38: D750-753

Nakazawa N, Arakawa O & Yanagida M (2019a) Condensin locates at transcriptional termination sites in mitosis, possibly releasing mitotic transcripts. *Open Biol* 9: 190125

Nakazawa N, Arakawa O & Yanagida M (2019b) Condensin facilitates sister chromatid separation in actively transcribed DNA regions by relieving the obstructive effect of transcription. bioRxiv 644799; doi: https://doi.org/10.1101/644799

Nakazawa N, Nakamura T, Kokubu A, Ebe M, Nagao K & Yanagida M (2008) Dissection of the essential steps for condensin accumulation at kinetochores and rDNAs during fission yeast mitosis. *J Cell Biol* 180: 1115–1131

Nakazawa N, Sajiki K, Xu X, Villar-Briones A, Arakawa O & Yanagida M (2015) RNA pol II transcript abundance controls condensin accumulation at mitotically up-regulated and heat-shock-inducible genes in fission yeast. *Genes Cells Devoted Mol Cell Mech* 20: 481–499

Naumova N, Imakaev M, Fudenberg G, Zhan Y, Lajoie BR, Mirny LA & Dekker J (2013) Organization of the mitotic chromosome. *Science* 342: 948–953

Noe Gonzalez M, Blears D & Svejstrup JQ (2021) Causes and consequences of RNA polymerase II stalling during transcript elongation. *Nat Rev Mol Cell Biol* 22: 3–21

Noma K, Cam HP, Maraia RJ & Grewal SIS (2006) A role for TFIIIC transcription factor complex in genome organization. *Cell* 125: 859–872

bioRxiv preprint doi: https://doi.org/10.1101/2020.11.13.381434; this version posted March 3, 2021. The copyright holder for this preprint (which was not certified by peer review) is the author/funder. All rights reserved. No reuse allowed without permission.

Petrova B, Dehler S, Kruitwagen T, Hériché J-K, Miura K & Haering CH (2013) Quantitative analysis of chromosome condensation in fission yeast. *Mol Cell Biol* 33: 984–998

Rivosecchi J, Larochelle M, Teste C, Grenier F, Malapert A, Ricci EP, Bernard P, Bachand F & Vanoosthuyse V (2019) Senataxin homologue Sen1 is required for efficient termination of RNA polymerase III transcription. *EMBO J* 38: e101955

van Ruiten MS & Rowland BD (2018) SMC Complexes: Universal DNA Looping Machines with Distinct Regulators. *Trends Genet TIG* 34: 477–487

Ryu J-K, Bouchoux C, Liu HW, Kim E, Minamino M, de Groot R, Katan AJ, Bonato A, Marenduzzo D, Michieletto D, *et al* (2021) Bridging-induced phase separation induced by cohesin SMC protein complexes. *Sci Adv* 7

Sakai A, Hizume K, Sutani T, Takeyasu K & Yanagida M (2003) Condensin but not cohesin SMC heterodimer induces DNA reannealing through protein-protein assembly. *EMBO J* 22: 2764–2775

Sakai Y, Mochizuki A, Kinoshita K, Hirano T & Tachikawa M (2018) Modeling the functions of condensin in chromosome shaping and segregation. *PLoS Comput Biol* 14: e1006152

Sheridan RM, Fong N, D'Alessandro A & Bentley DL (2019) Widespread Backtracking by RNA Pol II Is a Major Effector of Gene Activation, 5' Pause Release, Termination, and Transcription Elongation Rate. *Mol Cell* 73: 107-118.e4

Sigurdsson S, Dirac-Svejstrup AB & Svejstrup JQ (2010) Evidence that transcript cleavage is essential for RNA polymerase II transcription and cell viability. *Mol Cell* 38: 202–210

Sullivan NL, Marquis KA & Rudner DZ (2009) Recruitment of SMC by ParB-parS organizes the origin region and promotes efficient chromosome segregation. *Cell* 137: 697–707

Sutani T, Sakata T, Nakato R, Masuda K, Ishibashi M, Yamashita D, Suzuki Y, Hirano T, Bando M & Shirahige K (2015) Condensin targets and reduces unwound DNA structures associated with transcription in mitotic chromosome condensation. *Nat Commun* 6: 7815

Sutani T & Yanagida M (1997) DNA renaturation activity of the SMC complex implicated in chromosome condensation. *Nature* 388: 798–801

Toselli-Mollereau E, Robellet X, Fauque L, Lemaire S, Schiklenk C, Klein C, Hocquet C, Legros P, N'Guyen L, Mouillard L, *et al* (2016) Nucleosome eviction in mitosis assists condensin loading and chromosome condensation. *EMBO J* 35: 1565–1581

Tran NT, Laub MT & Le TBK (2017) SMC Progressively Aligns Chromosomal Arms in Caulobacter crescentus but Is Antagonized by Convergent Transcription. *Cell Rep* 20: 2057–2071

bioRxiv preprint doi: https://doi.org/10.1101/2020.11.13.381434; this version posted March 3, 2021. The copyright holder for this preprint (which was not certified by peer review) is the author/funder. All rights reserved. No reuse allowed without permission.

Uhlmann F (2016) SMC complexes: from DNA to chromosomes. *Nat Rev Mol Cell Biol* 17: 399–412

Vanoosthuyse V, Legros P, van der Sar SJA, Yvert G, Toda K, Le Bihan T, Watanabe Y, Hardwick K & Bernard P (2014) CPF-associated phosphatase activity opposes condensin-mediated chromosome condensation. *PLoS Genet* 10: e1004415

Vazquez Nunez R, Ruiz Avila LB & Gruber S (2019) Transient DNA Occupancy of the SMC Interarm Space in Prokaryotic Condensin. *Mol Cell* 75: 209-223.e6

Wang J, Pfeuty B, Thommen Q, Romano MC & Lefranc M (2014) Minimal model of transcriptional elongation processes with pauses. *Phys Rev E* 90: 050701

Wang X, Brandão HB, Le TBK, Laub MT & Rudner DZ (2017) Bacillus subtilis SMC complexes juxtapose chromosome arms as they travel from origin to terminus. *Science* 355: 524–527

Wang X, Le TBK, Lajoie BR, Dekker J, Laub MT & Rudner DZ (2015) Condensin promotes the juxtaposition of DNA flanking its loading site in Bacillus subtilis. *Genes Dev* 29: 1661–1675

Yanagida M (2009) Clearing the way for mitosis: is cohesin a target? *Nat Rev Mol Cell Biol* 10: 489–496

Zatreanu D, Han Z, Mitter R, Tumini E, Williams H, Gregersen L, Dirac-Svejstrup AB, Roma S, Stewart A, Aguilera A, *et al* (2019) Elongation Factor TFIIS Prevents Transcription Stress and R-Loop Accumulation to Maintain Genome Stability. *Mol Cell* 76: 57-69.e9

FIGURE LEGENDS

Figure 1: Distribution of condensin and RNAP2 upon flipping of *exg1*.
(A) ChIP-seq profiles of condensin (left) and the RNAP subunit Rpb5 (right) around *exg1* in mitotic cells. The ChIP-seq data are indicated by their SRA numbers and were generated in (Kakui *et al*, 2017) and (Sutani *et al*, 2015) respectively. (**B)** Cells were synchronized in mitosis and ChIP-qPCR in two different biological replicates was used to determine the distribution of condensin (left) and Rpb1 (right) around *exg1*. (**C)** Same as **(B)** when the orientation of *exg1* has been flipped over. The scheme above shows the organization of the chromosome around *exg1* in the wild-type (top) and in the reversed (bottom) orientations. Vertical dotted lines indicate the region of the chromosome that has been flipped over. Grey squares indicate the position of the *exg1* transcription unit. The % IP were normalized using the values given at the site within the gene body indicated by the red vertical dotted line (*exg1#1*). The raw data are shown in the source data files.

Figure 2: RNAP3 transcription defects induced by lack of Sen1 trigger the accumulation of condensin.
(A) Cells were synchronized in metaphase and the association of condensin (Cnd2-GFP) or the heterologous LacI (lacI-GFP) at the indicated loci was investigated by ChIP-qPCR in the presence and in the absence of Sen1 (mean ± std of 4 biological replicates; p-values determined by the test of Wilcoxon Mann-Whitney are indicated above the graph). **(B)** The association of the TFIIIC component Sfc6 at the indicated loci was investigated by ChIP-qPCR in cells synchronized in metaphase (mean ± std of 5 biological replicates). (**C,D).** Distribution

bioRxiv preprint doi: https://doi.org/10.1101/2020.11.13.381434; this version posted March 3, 2021. The copyright holder for this preprint (which was not certified by peer review) is the author/funder. All rights reserved. No reuse allowed without permission.

of condensin (cnd2-GFP, top) and RNAP3 (rpc37-flag, bottom) around *SPCTRNATHR.10* **(C)** and *SPCTRNAARG.10* **(D)** in mitotic cells, in the presence or not of super-terminator sequences (*thr10-20T* and *arg10-23T* respectively) which correct the transcription termination defects in the absence of Sen1 (Rivosecchi *et al*, 2019) (compare the yellow and red curves). Results are presented as (mean ± std) of 3 **(C)** or 4 **(D)** biological replicates.

Figure 3: The over-expression of *tfs1DN* alters significantly the distribution of condensin around RNAP2-transcribed genes.
Cells were synchronized in metaphase and the association of condensin (cnd2-GFP) at the indicated loci was investigated by ChIP-qPCR (mean ± std of 3 biological replicates). Cells carried a plasmid allowing the AhTET-induced over-expression of *tfs1-DN*, as described previously (Lemay *et al*, 2014). DMSO was used as control. For each locus investigated, the normal distribution of condensin and RNAP2 as determined by ChIP-seq is shown above, as published in (Kakui *et al*, 2017) and (Sutani *et al*, 2015) respectively. The data were normalized to the %IP at a site within the gene body indicated by the dotted line. The raw data are shown on Fig EV4.

Figure 4: Mathematical models formalize the role of RNAP backtracking in the specific accumulation of condensin in the termination zone of active genes.
(A) Interplay between the translocation of condensin and transcription - simple model (Brandão *et al*, 2019). Condensin translocates along chromatin from either 5' to 3' or 3' to 5'. RNAPs bind to TSS, translocate unidirectionally from 5' to 3' and unbind when they reach the termination zone. The speed at which condensin translocates is reduced when it encounters a RNAP. Moving RNAPs can push condensin towards the 3' of the gene if they represent an obstacle for their translocation (see Methods and Supplementary Text). **(B)** Profile of RNAP mimicking a typical WT-situation of a ~2kbp-long gene (see for example Figures 1&3). **(C)** Residence time profiles of condensin along the gene when condensin and RNAP move in the same (head-to-tail, full lines) or opposite (head-to-head, dashed lines) direction for two different bypassing rates. **(D)** Interplay between the translocation of condensin and transcription - backtrack model. This model makes the same basic assumptions as in **(A)** but RNAP can now dynamically switch between two states: either mobile (mRNAP) or backtracked (bRNAP). The reduction in condensin speed due to collisions with RNAP is stronger with bRNAP than with mRNAP (see Methods and Supplementary Text). **(E)** Rate of backtracking along the gene used in the model. **(FG)** Wild-type situation. **(F)** Density of total RNAP (black line) and bRNAPs (red line) over a ~2kbp-long gene. **(G)** Residence time profiles of condensin along the gene for head-to-tail (full black line) or head-to-head (dashed black line) collisions for a fast bypass rate over mobile RNAP (15bp/s). The blue full line represents the average between both profiles. **(HI)** Over-expression of *tfs1DN*. **(H)** Profiles of RNAP (black line) and backtracked RNAPs (red line) obtained by increasing the dwell-time of the backtracked state by 10-fold to mimic the *tfs1DN* situation. **(I)** As in **(G)** but for the *tfs1DN-like* simulations.

Supplementary Figure 1: Lack of Sen1 does not significantly alter the association of Tbp1 at RNAP3-transcribed genes. Cells were synchronized in metaphase by depleting Slp1 (see Methods). The association of Tbp1 at the indicated loci was investigated by ChIP-qPCR (mean ± std of 4 biological replicates).

Supplementary Figure 2: The over-expression of *tfs1DN* does not interfere with the occupancy of condensin at the rDNA. The samples described in Fig 3 were used to monitor the occupancy of condensin within the RNAP1-transcribed 18S transcription unit.

Supplementary Figure 3: Mathematical model of the interplay between the translocation of condensin and immobile obstacles bound to chromatin. (A) Condensin translocates along chromatin from either 5' to 3' or 3' to 5' at a fast rate (~1kbp/s). When it encounters an obstacle bound to chromatin, its translocating speed is strongly reduced (~10bp/s). Obstacles can dynamically bind and unbind to chromatin with a typical life-time of 1 minute. Simulations

bioRxiv preprint doi: https://doi.org/10.1101/2020.11.13.381434; this version posted March 3, 2021. The copyright holder for this preprint (which was not certified by peer review) is the author/funder. All rights reserved. No reuse allowed without permission.

of this stochastic system were done using Gillespie simulations as for the models described in Fig.4AD (see Materials and Methods of the main text). **(B)** Two toy examples of obstacle occupancy. **(C)** The residence time of condensin at a given position follows the profile of obstacles occupancy and is symmetric regarding the directionality of condensin.

Supplementary Figure 4: Analysis of the simple and backtrack models. (A) RNAP occupancy predicted by the simple model ($\gamma_{term} = v_c = 0.4$ s^{-1}) for two different values of the initiation rate γ_{init}. **(B)** Profiles of residence time in the simple model for condensins translocating from 5' to 3' (head-to-tail, full lines) or from 3' to 5' (head-to-head, dashed lines) for both γ_{init} values shown in (A) (red & black for $\gamma_{init} = 0.05$ s^{-1}, blue & yellow for $\gamma_{init} = 0.025$ s^{-1}) and for two values of the bypassing rate v_{jump} (black & blue for a 'fast' rate, red & yellow for a 'slow' rate). The inset magnifies the profiles for the higher v_{jump} value. **(C)** RNAP occupancy predicted by the backtrack model ($\gamma_{term} = v_c = 0.4$ s^{-1}, $\gamma_{init} = 0.05$ s^{-1}) for 'slow' (full lines) or 'fast' (dashed lines) switching rates k_{on} and $k_{back,min}$. Black lines represent the full RNAPs occupancy while the red lines only the bRNAPs. **(D)** Profiles of residence time for condensins translocating from 5' to 3' (head-to-tail, full lines) or from 3' to 5' (head-to-head, dashed lines) for parameters corresponding to RNAPs profiles shown in (C) (red & black for 'slow' switching rates, blue & yellow for 'fast' switching rates) and for two values of the bypassing rate v^m_{jump} (v^b_{jump}=0) (black & blue for a 'fast' rate, red & yellow for a slower rate). The inset magnifies the profiles for the higher v^m_{jump} value. **(E)** As in (C) but for ($v_c = 0.4$ s^{-1}, $\gamma_{init} = 0.05$ s^{-1}, $\gamma_{term} = 0.2$ s^{-1}). **(F)** As in (D) but for the parameters corresponding to RNAPs profiles shown in (E). All profiles correspond to v^b_{jump}=0, except the green lines in the inset with v^b_{jump}=10 bp/s. **(G)** Total RNAPs (black lines) or bRNAPs (red lines) profiles for *tfs1DN*-like situations in the case of 'slow' switching rates ($k_{back,min} = 0.002$ s^{-1}) for different changes in the k_{on} value (full line=WT-like situation as in (E)). **(H)** As in (G) but in the case of 'fast' switching rates ($k_{back,min} = 0.1$ s^{-1}). **(I)** Profiles of residence time for condensin translocating from 5' to 3' (head-to-tail, full lines) or from 3' to 5' (head-to-head, dashed lines) for parameters corresponding to the dashed and dotted profiles shown in (G) (slow switching rate regime) and for a 'fast' bypassing rate v^m_{jump} (v^b_{jump}=0).

Supplementary Table S1: Fission yeast strains used in this study

Supplementary Table S2: Primers used in this study

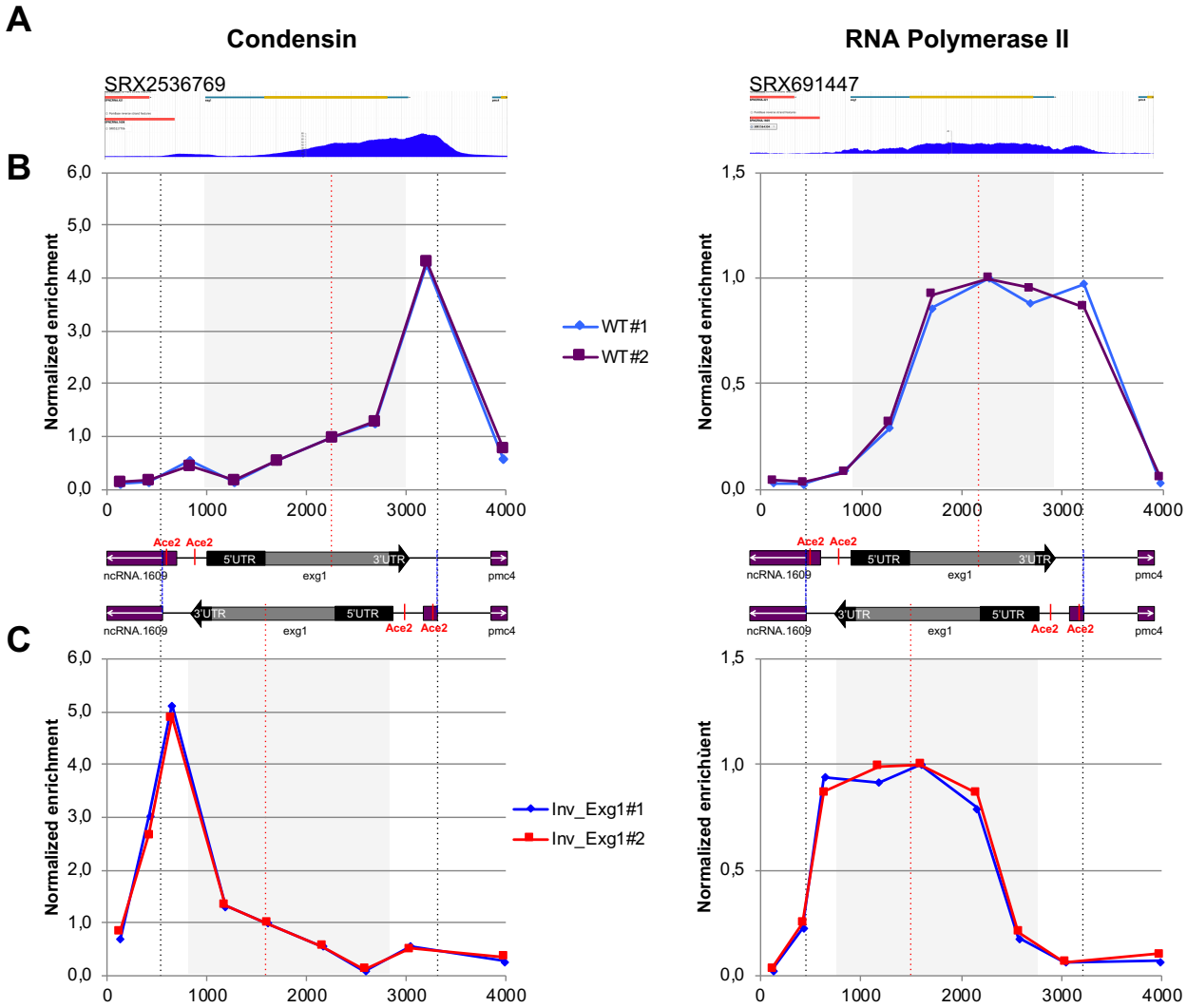
A
Condensin
RNA Polymerase II
SRX2536769
SRX691447
B
Normalized enrichment
WT#1
WT#2
Ace2 Ace2
5'UTR
3'UTR
ncRNA.1609
exg1
pmc4
C
Inv_Exg1#1
Inv_Exg1#2

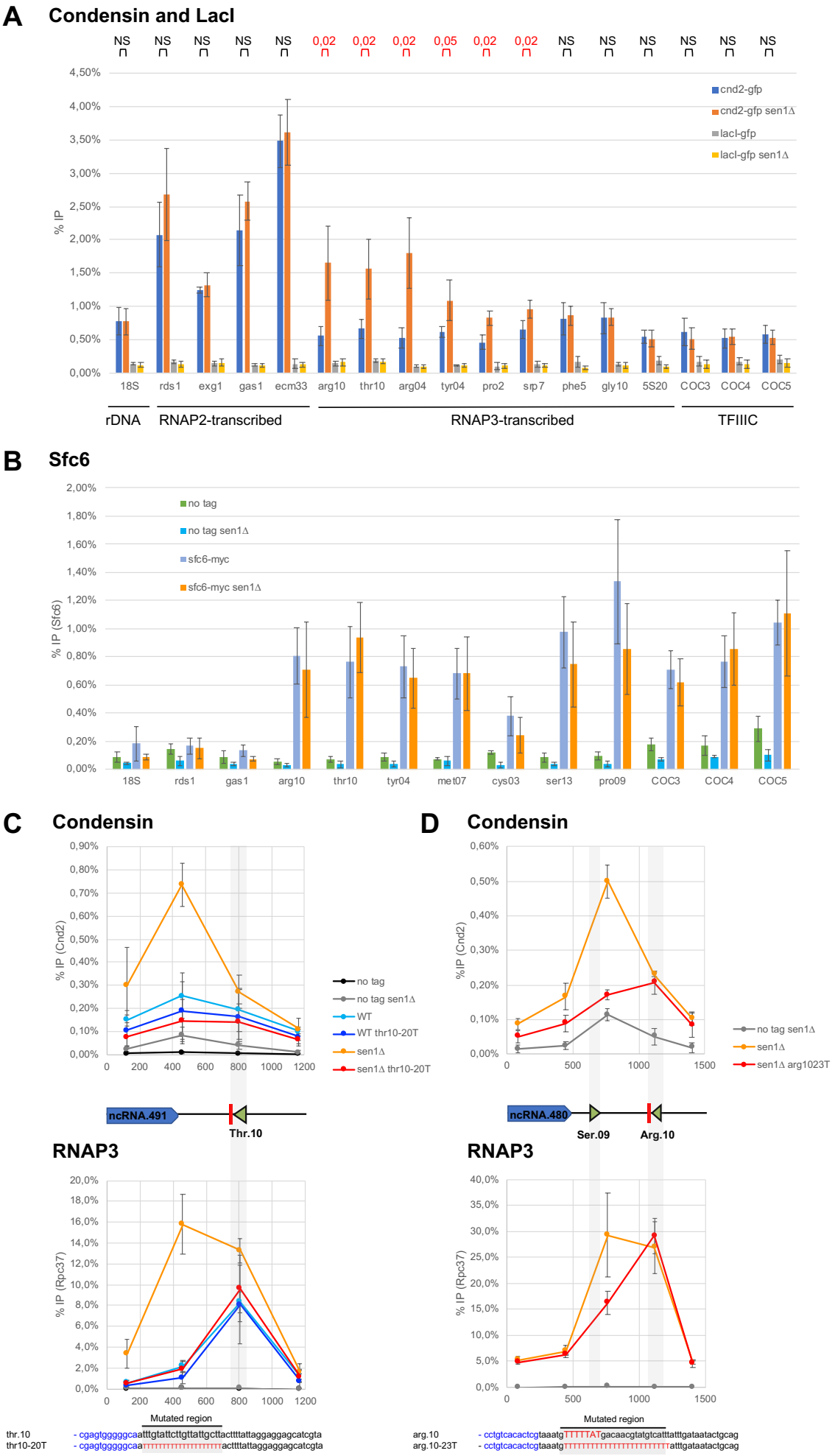
A
Condensin and LacI
NS NS NS NS NS 0,02 0,02 0,02 0,05 0,02 0,02 NS NS NS NS NS NS
% IP
cnd2-gfp
cnd2-gfp sen1Δ
lacI-gfp
lacI-gfp sen1Δ
18S rds1 exg1 gas1 ecm33 arg10 thr10 arg04 tyr04 pro2 srp7 phe5 gly10 5S20 COC3 COC4 COC5
rDNA
RNAP2-transcribed
RNAP3-transcribed
TFIIIC
B
Sfc6
% IP (Sfc6)
no tag
no tag sen1Δ
sfc6-myc
sfc6-myc sen1Δ
18S rds1 gas1 arg10 thr10 tyr04 met07 cys03 ser13 pro09 COC3 COC4 COC5
C
Condensin
% IP (Cnd2)
no tag
no tag sen1Δ
WT
WT thr10-20T
sen1Δ
sen1Δ thr10-20T
ncRNA.491
Thr.10
RNAP3
% IP (Rpc37)
Mutated region
thr.10 - cgagtgggggcaatttgtattcttgttattgcttacttttattaggaggagcatcgta
thr10-20T - cgagtgggggcaarrrrrrrrrrrrrrrrrrrrrractttattaggaggagcatcgta
D
Condensin
%IP (Cnd2)
no tag sen1Δ
sen1Δ
sen1Δ arg1023T
ncRNA.480
Ser.09
Arg.10
RNAP3
% IP (Rpc37)
Mutated region
arg.10 - cctgtcacactcgtaaatgTTTTTATgacaacgtatgtcatttatttgataatactgcag
arg.10-23T - cctgtcacactcgtaaatgrrrrrrrrrrrrrrrrrrr

Rivosecchi. Figure 3.

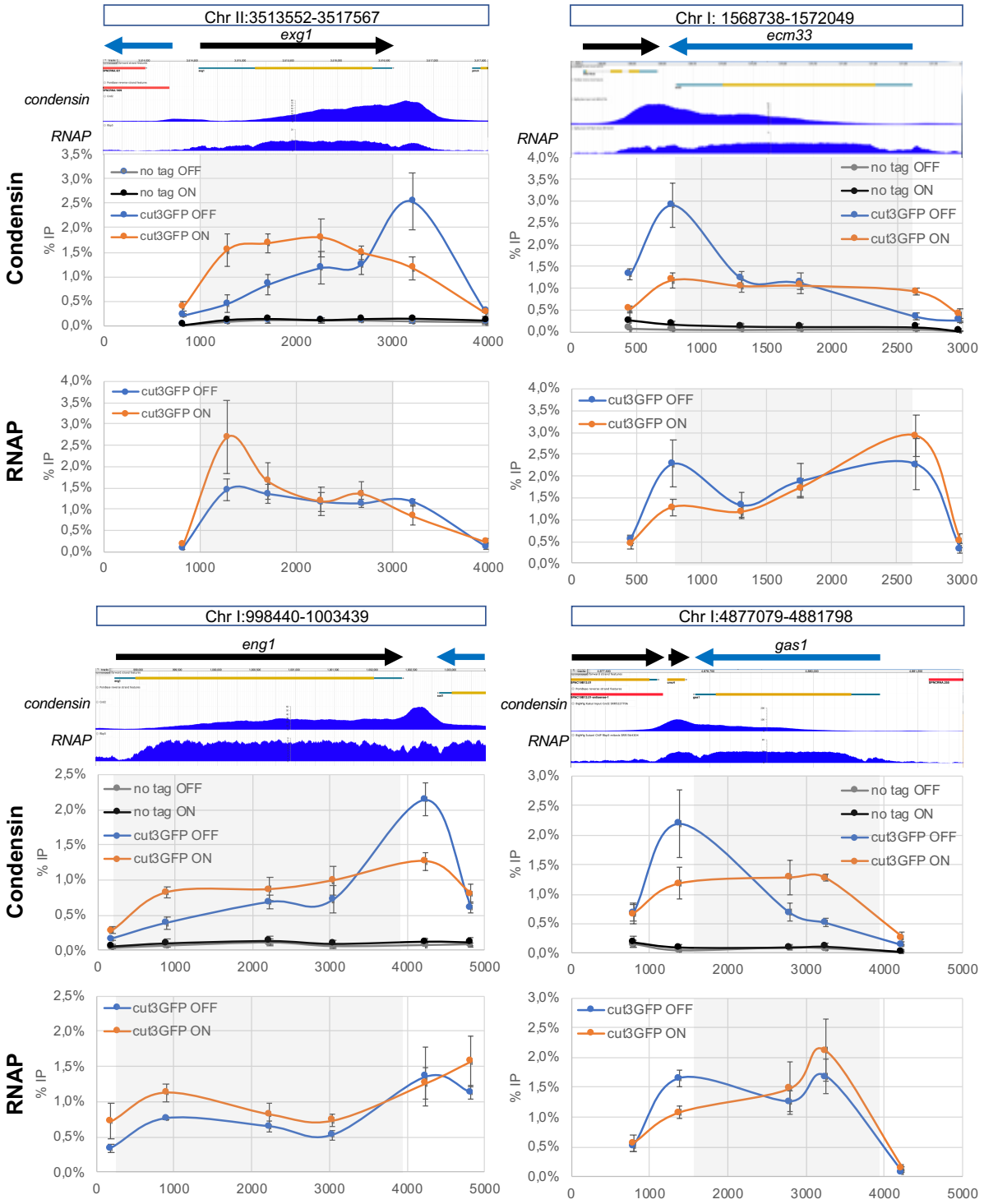

Rivosecchi. Figure 4

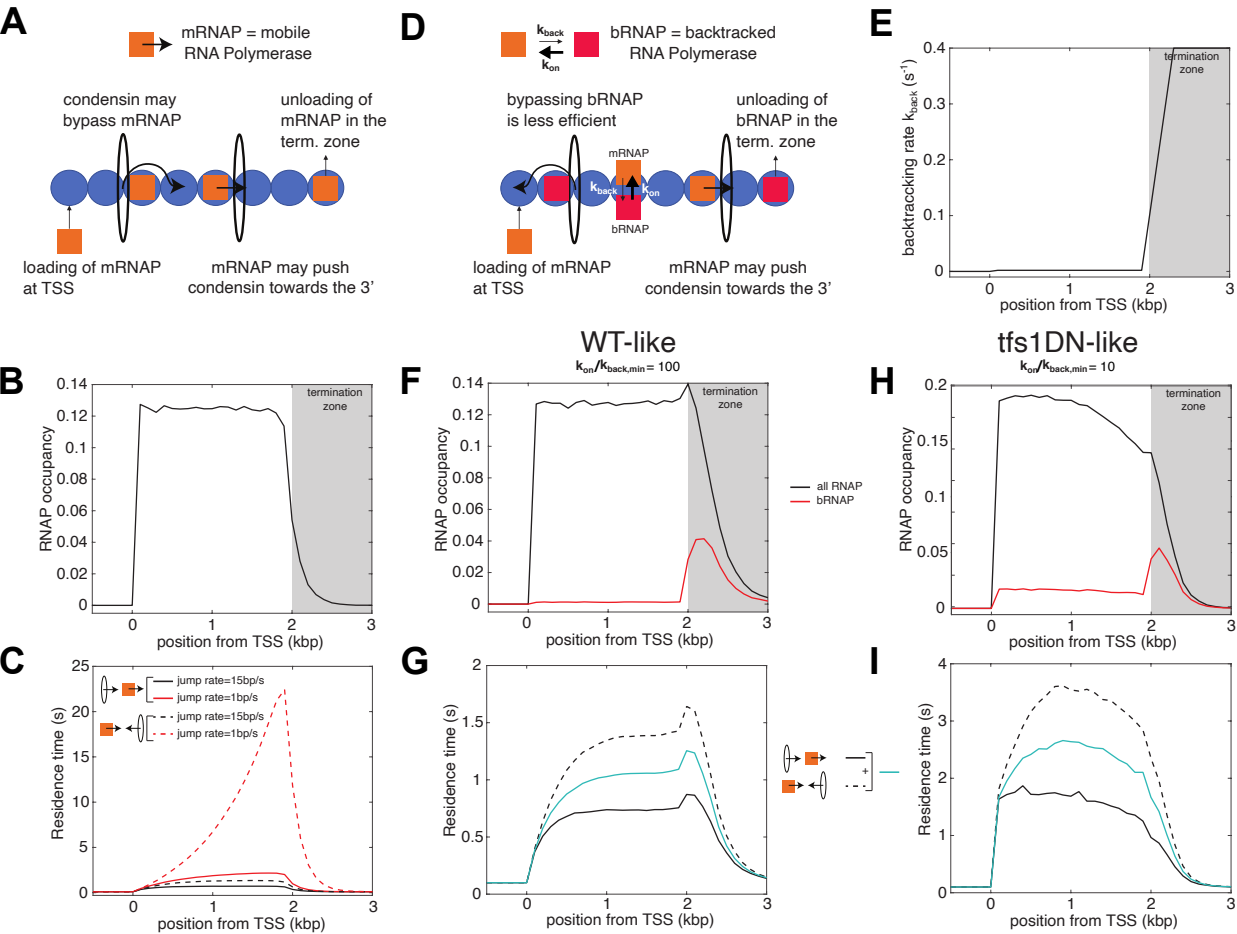

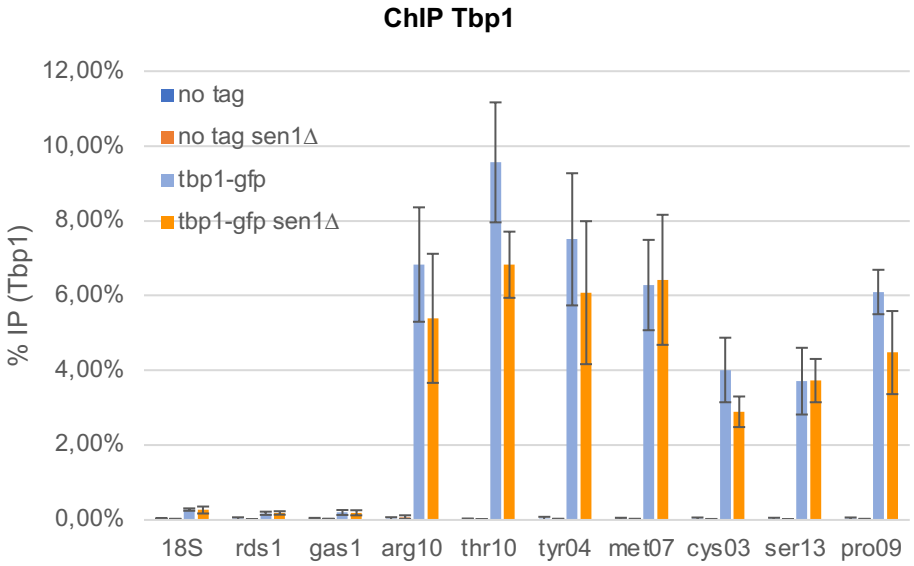
ChIP Tbp1
12,00%
10,00%
8,00%
6,00%
4,00%
2,00%
0,00%
% IP (Tbp1)
no tag
no tag sen1Δ
tbp1-gfp
tbp1-gfp sen1Δ
18S
rds1
gas1
arg10
thr10
tyr04
met07
cys03
ser13
pro09

Rivosecchi. Supplementary Figure S2

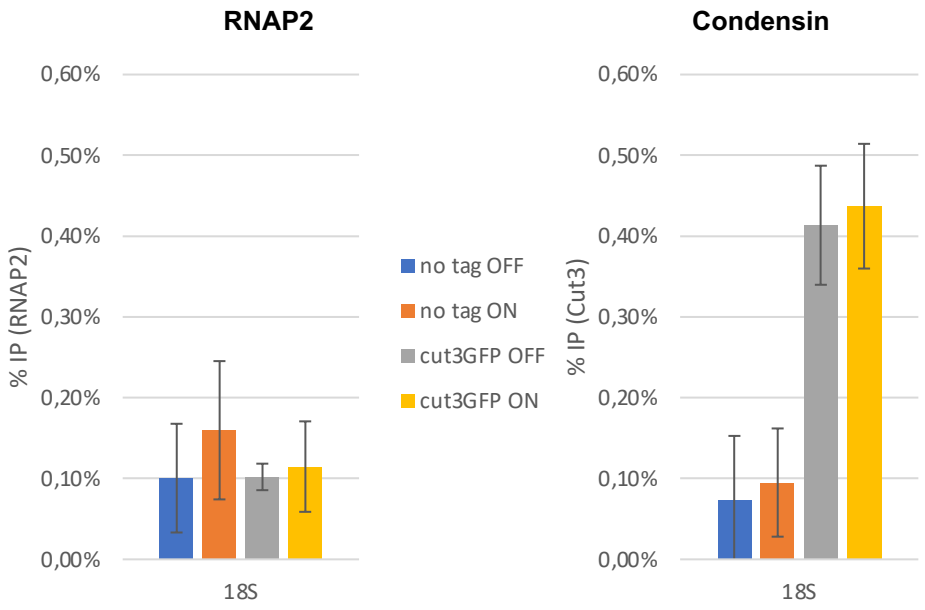

Rivosecchi. Supplementary Figure S3

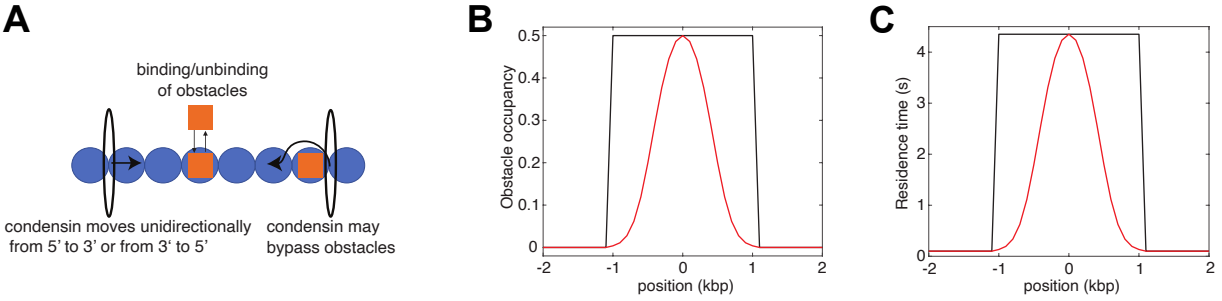

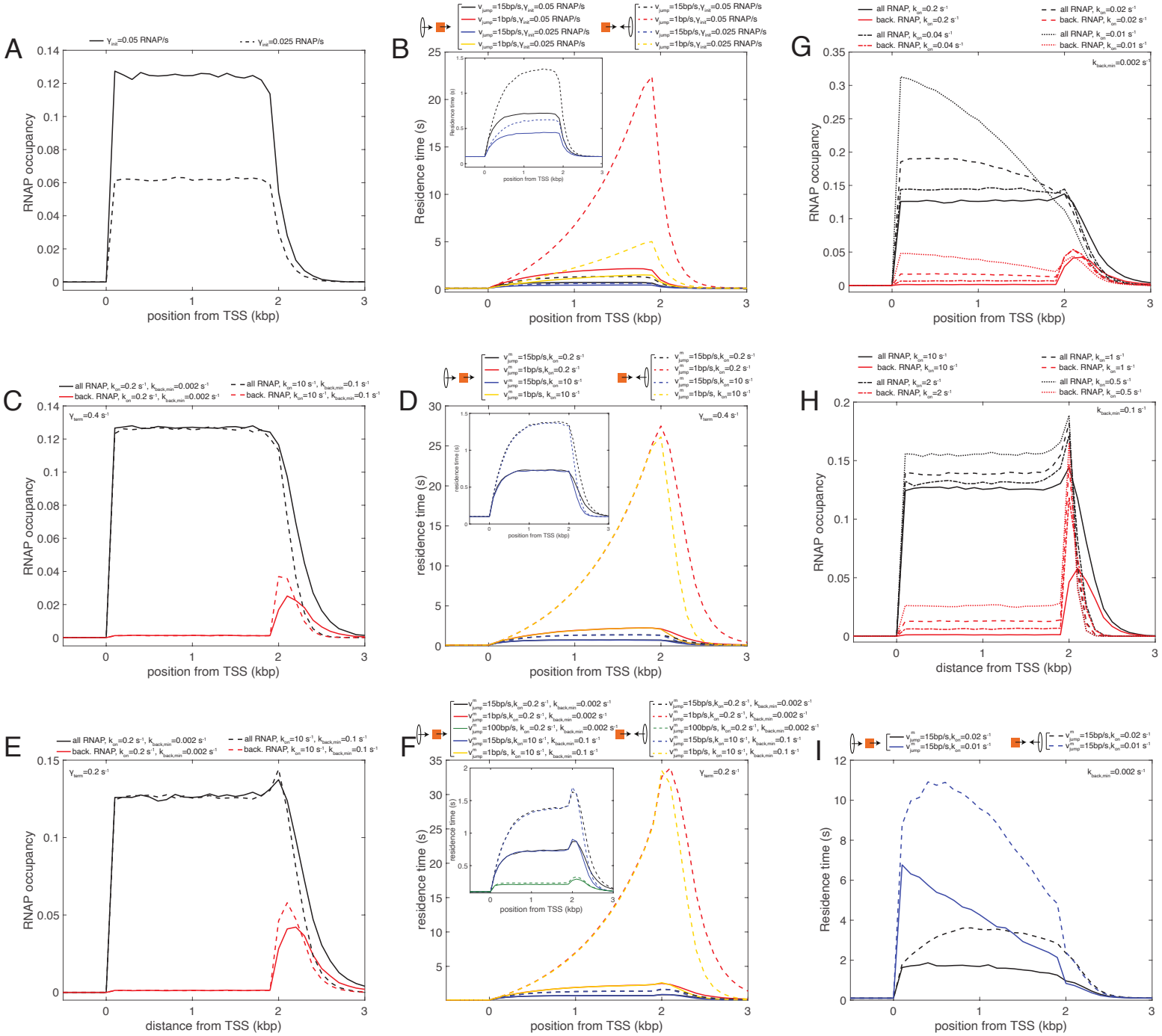

Rivosecchi. Supplementary Fig S4

Supplementary Text

Simple model (Supplementary Fig S4A-B). The model used to describe RNA elongation is a simple TASEP (Derrida *et al*, 1992). In this framework, flat, WT-like, profiles may be obtained by equating the speed rate of translocating agents and the termination rate ($\gamma_{term} = v_c$), the initiation rate (γ_{init}) controlling the global density of agents in the region (Supplementary Fig S4A). As already observed in (Brandão *et al*, 2019), profiles of residence time of condensin along the gene depend on the direction of condensin translocation (Supplementary Fig S4B). (1) When condensin and RNAP move in the same direction (full lines in Supplementary Fig S4B), head-to-tail collisions between both motors may occur. RNAPs then act as obstacles and slow down condensin movement. The shapes of the condensin residence profiles thus mostly follow the flat distribution of RNAP. The slowing-down of condensin is more important for genes denser in RNAPs (compare black & red full lines with blue & yellow full lines) and for lower bypassing rates (compare black & blue full lines with red & yellow full lines). (2) When condensin and RNAP move in opposite directions (dashed lines in Supplementary Fig S4B), head-to-head collisions occur. If the bypass rate of condensin over RNAP is fast enough, RNAPs represent mainly obstacles as in the head-to-tail case (black & blue dashed lines). For slow bypass rates (red & yellow dashed lines), RNAPs translocation forces condensin to move back leading to a dramatic gain in the residence time with increasing, super-linear, profiles along the gene. Regions denser in RNAPs show stronger effects. In both (head-to-tail, head-to-head) situations, residence profiles do not capture the overall shape of experimental condensin profiles observed in WT that exhibit a slow, gradual increase along the gene body followed by a strong accumulation closed to the transcription termination site (Fig 3).

Backtrack model (Supplementary Fig S4C-I). We assumed (i) that the backtracking rate is much stronger in the termination zone ($k_{back,min} \equiv k_{back}(gene\ body) = k_{back}\ (termination\ zone)/200$, Fig 4E), (ii) that the proportion of backtracked RNAPs (bRNAPs) in the gene body is very low ($k_{on}/k_{back,min} = 100$) in WT, and (iii) that the effect of bRNAPs on the translocation of condensin is maximal ($v^b_{jump} = 0$). Applying the same TASEP parameters as in the simple model ($\gamma_{term} = v_c$ =0.4 s^{-1}), we also observed flat profiles for RNAP (black lines in Supplementary Fig S4C) and we observed that bRNAPs mostly accumulate at the termination zone (red lines in Supplementary Fig S4C), with very similar behaviours whether the switching rates k_{on} and $k_{back,min}$ are 'fast' (dashed lines) or 'slow' (full lines). However, the density of bRNAPs is not strong enough to strongly influence the translocation of condensins and the system mainly behaves like in the simple model (Supplementary Fig S4D), independently of the kinetics of switching. To increase the number of bRNAPs in the termination zone while maintaining a nearly flat profile for RNAP along the gene (with a minimal change in the parameters), we reduced the unbinding rate γ_{term} to 0.2 s^{-1}, stabilizing more bRNAPs at the termination zone (Supplementary Fig S4E). When the bypassing rate v^m_{jump} over mobile RNAPs (mRNAPs) is fast enough, head-to-tail (black & blue full lines in Supplementary Fig S4F) and head-to-head (black & blue dashed lines) situations lead to similar shape in residence time with a flat or slightly increasing profile in the gene body (following the overall RNAPs density) followed by a sudden increased at the termination zone (as observed experimentally) due to the stronger speed reduction imposed by bRNAPs. When v^m_{jump} is too small (red & yellow lines in Supplementary Fig S4F), the difference in bypassing rates between mRNAPs and bRNAPs is weak and the system behaves almost as in the simple model with low bypassing rates. Both behaviours (high vs low v^m_{jump}) persist for fast or slow switching rates (compare red & black with blue & yellow lines in Supplementary Fig S4F). Note that in order to observe a WT-like profile for condensin residence time, v^b_{jump} does not necessarily need to be equal to zero, but the difference between v^m_{jump} and v^b_{jump} has to be large enough to differentiate the effect of mRNAPs and bRNAPs (green lines in the inset of Supplementary Fig S4F). In the model, the *tfs1DN* situation was mimicked by increasing the dwell time ($\sim 1/k_{on}$) of the backtracked state. In order to obtain a tilted RNAP profile as

observed experimentally (Fig 3), we found that the switching rates k_{on} and k_{back} have to be 'slow' (compare black lines in Supplementary Fig S4G for 'slow' rates with black lines in Supplementary Fig S4H for 'fast' rates) and the increase in the life-time of the bRNAP state has to be strong enough ($k_{on}(WT)/\, k_{on}(tfs1DN) \gtrsim 8$) (dotted and dashed black lines in Supplementary Fig S4G), as the tilted profile emerges from the formation of transient traffic jams generated by paused RNAPs with sufficiently large dwell-times. This leads to a significant increase of the bRNAPs density inside the gene body compared to the WT-like situation (red dashed and dotted lines in Supplementary Fig S4G). These changes in RNAP and bRNAPs profiles lead to the loss of the high condensin occupancy at the 3' of the gene and to an overall flattening of the residence time (black lines in Supplementary Fig S4I) if the stabilization of bRNAPs is not too strong and the corresponding RNAPs profiles are not too tilted (blue lines in Supplementary Fig S4I).

Supplementary References.

Brandão HB, Paul P, van den Berg AA, Rudner DZ, Wang X & Mirny LA (2019) RNA polymerases as moving barriers to condensin loop extrusion. *Proc Natl Acad Sci USA* 116: 20489–20499

Derrida B, Domany E & Mukamel D (1992) An exact solution of a one-dimensional asymmetric exclusion model with open boundaries. *J Stat Phys* 69: 667–687